

# In Vitro Calcium Dissolution Behavior of Hydroxyapatite Coatings with Different Characteristics

Z. Mohammadi, A. A. Ziae-Moayyed, A. S. Mesgar

Materials Science and Engineering Department, Sharif University of Technology, Tehran, Islamic Republic of Iran

e-mail: mohamadiz@mehr.sharif.edu

**Abstract-**The calcium dissolution behavior of plasma sprayed hydroxyapatite (HA) coatings with different characteristics, deposited on the Ti alloy using various process parameters, in the simulated body fluid (SBF) were evaluated. The residual stress, porosity, surface roughness and crystallinity of the HA coatings were determined experimentally using the indentation technique, the Archimedian method, the surface profilometry technique, and XRD method. Measurement of calcium ion concentration in dissolution testing in SBF solution for 1 and 3 days revealed an enhancing influence of the porosity, the residual stress and the surface roughness, along with an impeding effect of the crystallinity on the dissolution of the coatings. It was found that the presence of tensile residual stress in the HA coatings significantly increases the rate of dissolution at initial times of dissolution. The combined effect of surface roughness, porosity, residual stress and crystallinity determines the dissolution behavior of the HA coatings. It was deduced that for both to promote a rapid integration and the long-term stability of coatings, it is desirable to produce coatings with a low tensile residual stress, or under zero stress conditions.

**Keywords:** *In vitro dissolution; Residual stress; plasma spray; Hydroxyapatite;*

## I. INTRODUCTION

Hydroxyapatite (HA) coatings deposited on metal implants have been used to improve fixation of prosthetic appliances due to their excellent biocompatibility and bone-bond ability [1],[2]. It is suggested that an ideal HA coating for orthopedic cementless implants would be one with a high chemical stability, phase purity, low porosity, a high surface roughness and strong cohesive and adhesive properties [3]. These considerations are taken to reach the long-term stability and/or the promotion of a rapid integration of implant to bone.

It is recognized that the presence of calcium ions in moderate amounts at the implant-tissue interface promotes bone remodeling [4]. However, excessive levels of dissolution products give rise to cytotoxic effects on bone cells, due to driving up the local pH values [5]. On the base of these findings, it is suggested that the short-term release of ions from dissolving HA coatings must be minimized [4].

It is believed that in addition to phase composition and crystal size, the coating characteristics, such as surface roughness, porosity, actual surface area, morphology and residual stress would influence dissolution of coatings [6]. The porosity controls the surface area in contact with body fluid [1] and, therefore, influences dissolution of the coatings. The surface roughness of HA coatings plays an important role in optimum growth of bone trabeculae [4]. Its higher value is favorable for the cell anchorage [7]. It is reported that the

presence of residual stress can enhance or impede dissolution of the coating [8].

The objective of this work was to study the relationship between the four coating characteristics (i.e. porosity, surface roughness, residual stress and crystallinity) and the early calcium dissolution behavior of HA coatings in SBF. To achieve this, nine HA coatings deposited at different spraying conditions were used.

## II. MATERIALS AND METHODS

The grit-blasted plates of Ti-6Al-4V alloy (13 mm × 13 mm × 2 mm) with an average surface roughness ( $R_a$ ) of 3.5 μm were used as substrates. A commercial high purity HA powder (CAPTAL 60, Plasma Biotal Limited, UK) was used as starting powder. Nine different samples of HA coatings were prepared using a METCO 3MB plasma spray system by adjusting the input power level and the spray distance (SD) (Table 1). Argon was used both as the primary gas (at 50 slpm) and carrier gas (at 3.78 slpm). Hydrogen selected as the secondary gas (at 10 slpm). The transverse speed of the plasma gun was set at 250 mm s<sup>-1</sup>. HA coatings with an average thickness of 200 ± 20 μm were deposited on the roughened substrates.

The crystallinity was evaluated from the main peak ratio,  $I/I_{HA}$ , base on a relative method [9], where  $I$  is the main peak height of HA on the XRD pattern of the coating and  $I_{HA}$  is the main peak height of HA on the XRD pattern of the powder. The HA powder considered as a material of 100 % crystallinity. The degree of crystallinity (DOC) was defined as follows:

$$\text{DOC} (\%) = \frac{I}{I_{HA}} \times 100 \quad (1)$$

Porosity of the peel-off coatings was measured by using Archimedean method based on the procedure suggested by Mancini et al [10]. Three samples were tested for each condition.

The surface roughness ( $R_a$ ) of coatings was measured using a surface profilometry technique (SURFOMETER model SF200). Average value of  $R_a$  was determined using five measurements per each sample.

The coating surfaces were characterized using a scanning electron microscopy (JXA-840, JEOL Scanning Micro-analyzer).

Residual stress of the coatings ( $\sigma$ ) was estimated by Vickers indentation method using the following equation [11], [12]:

$$K_{IC} = 0.016 \left[ \frac{P}{C^{3/2}} \right] \left[ \frac{E}{H} \right]^{1/2} + \beta \sigma C^{1/2} \quad (2)$$

where  $P$  is the applied load,  $C$  is the crack length ahead of diagonal of indentation,  $\beta$  is a shape factor, which takes a value of 1.26 for semi-circular surface cracks, and  $K_{IC}$  is the fracture toughness. The ratio of  $H/E$  was estimated by Knoop indentation method. The residual stress was determined by plotting the indentation stress intensity,  $0.016 (P/C^{3/2}) (E/H)^{1/2}$ , against the residual stress intensity,  $\beta C^{1/2}$ . The Vickers hardness of coatings was measured at various cross-sectional positions using a Uniteck hardness tester with a load of 50 gf and a loading time of 15 s. The average result of ten indentations was considered as the micro-hardness.

The evaluation of dissolution behavior was made by measuring the concentration of calcium ion released into the simulated body fluid (SBF) solution at 37 °C for 1 and 3 days using Inductively Coupled Plasma Atomic Emission Spectroscopy (ICP, ARL 3410).

### III. RESULTS AND DISCUSSION

The XRD patterns of the HA powder and three HA coatings (i.e. A1, A5, A9) are shown in Fig. 1. It reveals that the feedstock powder is a high purity HA (Fig. 1a). Fig. 1b shows that the HA coatings are mainly composed of HA and impurity phases. The high temperature of plasma flame transformed the crystalline HA into a mixture of HA and impurity phases (i.e. tricalcium phosphates ( $Ca_3(PO_4)_2$ ),  $\alpha$ -TCP,  $\beta$ -TCP), tetracalcium phosphate ( $Ca_9P_2O_{10}$ , TTCP), calcium oxide (CaO) and an amorphous calcium phosphate phase (ACP). When either the spray power or SD was increased, the intensity of HA peaks decreased, but the amount of impurity phases increased.

Table 1 shows the degree of crystallinity (DOC) of all the HA coatings. It indicates that the crystallinity decreased with increasing the spray power and SD. An increase in spray power usually leads to the lower crystallinity because of more melting of particles due to the higher temperature of both the plasma flame and the particles [13]. On the other hand, more melting of the particles due to longer residence time, and decreased substrate and incoming droplets temperature are the reasons for decrease of crystallinity at longer SD [13].

The percent of apparent porosity of the samples is also shown in Table 1. The results are usually consistent with DOC results; i.e. the lower the crystallinity, the lower the porosity. The formation of more amorphous phase due to an increase of spray power and/or SD give rise to better filling of the pores between splats and decrease of the porosity.

Fig. 2 shows the surface morphologies of the coatings. The morphology of coating A1 with the highest crystallinity mainly consisted of unmelted and partially melted particles, which indicates insufficient melting of the particles (Fig. 2a). The coating A7 exhibited enhanced particle melting due to a higher plasma temperature, as a result of increasing spray power (Fig. 2c). The morphology of coating A5 was mainly composed of flattened splats and partially melted particles being embedded in the flattened splats (Fig. 2b). The coating A9 with the lowest crystallinity and porosity showed a surface morphology mainly consisted of well-flattened splats as well as some partially melted particles due to a higher

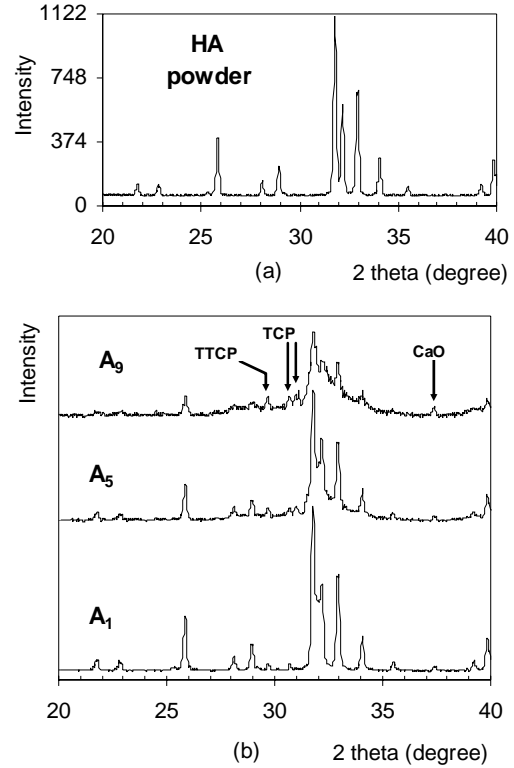


Fig.1. XRD patterns of (a) HA powder and (b) plasma sprayed hydroxyapatite coatings.

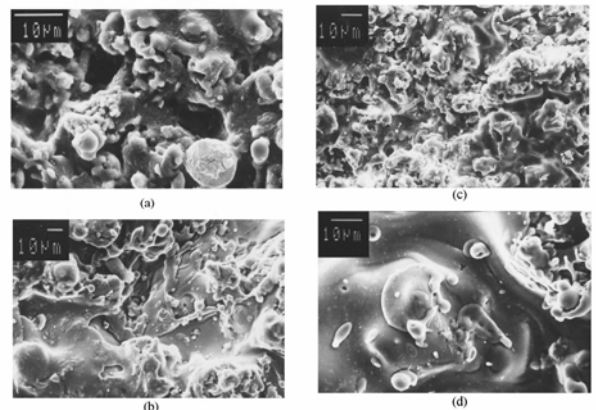


Fig. 2. Surface morphology of the HA coatings  
(a) A1, (b) A5, (c) A7, (d) A9.

plasma temperature and a longer meting period (Fig. 2d). The average surface roughness values of the HA coatings are shown in Table 1. The results indicate that the surface roughness of HA coatings which reflects the irregular morphology of their surfaces is not consistent with the previous DOC results. It is expected that the coatings with lower crystallinity would have a smoother surface. It is believed that the spraying at longer SD usually reduces the velocity of the droplets [13]. The spraying of droplets with a reduced velocity results in their less spreading when the droplets deposit on the previous layers. On the other hand, It is reported that de-agglomeration of the unmelted or partially

TABLE 1  
Spraying conditions of the samples with their characteristics values

	A <sub>1</sub>	A <sub>2</sub>	A <sub>3</sub>	A <sub>4</sub>	A <sub>5</sub>	A <sub>6</sub>	A <sub>7</sub>	A <sub>8</sub>	A <sub>9</sub>
<b>Spray condition</b>									
Power (kW)/SD (mm)	28.0/80	28.0/110	28.0/140	32.2/80	32.2/110	32.2/140	36.4/80	36.4/110	36.4/140
DOC (%)	61.7	51.2	40.3	60.1	48.7	36.5	58.1	45.1	32.5
P (%)	10.7±2.0	7.9±1.2	5.0±0.8	10.1±2.1	7.6±1.2	5.2±0.9	9.1±1.9	7.2±1.3	5.4±0.9
R <sub>a</sub> (μm)	8.7±1.6	10.1±1.5	11.5±1.2	10.6±1.2	11.5±2.0	11.7±1.8	12.5±1.5	12.2±2.0	11.7±1.6
σ (MPa)	21.5	20.3	16.9	42.1	34.7	33.7	61.4	52.5	46.8
Ca (mM) 1 day	3.30	3.34	3.38	3.59	3.57	3.55	3.85	3.75	3.68
Ca (mM) 3 days	3.85	3.96	4.09	3.94	4.04	4.14	4.01	4.11	4.19

melted particles in plasma flame can be occur at longer SD when each particle agglomerated by many primary particles [13]. The spraying at a higher power level usually increases the plasma temperature. In this work, the plasma power level was increased by increasing arc current which controls directly the in-flight particle characteristics increasing their temperature and velocity [14]. An increase in plasma temperature enhances particle melting and spreading. However, an increase in the velocity of particles can lead to de-agglomerate some of the unmelted or partially melted particles when the particles impacted on the substrate. The above-mentioned effects which can determine the dominated morphology of the coatings may control the surface roughness. This indicates that the surface roughness depends on the morphological features of the coatings which in turn relate to the particles melting and droplets spreading.

The residual stress usually varies with spraying parameters, cooling conditions and coating thickness. Thus, the differences in the resulting residual stress of the HA coatings may be attributed to the differences in the temperature of the coatings relative to substrate during plasma spraying due to variations in spraying parameters. The residual stress increases with increasing the temperature of coating. Therefore, it would be expected that the coatings deposited at higher plasma power or at shorter spray distance would exhibit higher residual stress. The results, as indicated in Table 1, reveal that the residual stresses measured on the cross section of the HA coatings by the indentation method were in the tensile state. This may be attributed to the coefficient of thermal expansion (CTE) of HA which is higher than that of the Ti-6Al-4V substrate ( $\alpha_{\text{Ti-6Al-4V}} = 8.9 \times 10^{-6} \text{ K}^{-1}$ ,  $\alpha_{\text{HA}} = 11.5 \times 10^{-6} \text{ K}^{-1}$ ). It is noted that the residual stress in plasma sprayed ceramic coatings are generally classified as quenching stresses arising from impact, spreading and solidification of each droplet on the substrate surface, and differential thermal contractions (DTC) stresses originating from CTE mismatch between coating and substrate [15]. The quenching stresses are always tensile [3,15]. This indicates that the residual stress in the HA coatings would be in the tensile state.

Table 1 also shows the concentration of calcium ion released into the SBF solution from the HA coatings after

immersion for 1 and 3 days. As discussed previously, the spraying at a higher spray power and /or SD leads to decrease crystallinity and purity of HA. Since the impurity phases dissolve more rapidly compared to HA in order CaO >> TTCP > ACP > TCP >> HA [4], it would be expected that the coatings with a lower crystallinity exhibit higher calcium concentrations released to the solution.

In an attempt to interpret the calcium concentration as a function of DOC, a difficulty arises since the former after 1 or 3 days incubation is not consistent with the latter. This behavior indicates that the three other coating characteristics; i.e. roughness, residual stress and porosity, may influence the dissolution of HA coatings. The order of these characteristics was also not consistent with the solubility after 1 or 3 days incubation. Therefore, the resulting calcium concentration was determined by a combined effect of these characteristics and the crystallinity.

The calcium concentrations after 1 and 3 days incubation ( $C_{\text{Ca}}^1$  and  $C_{\text{Ca}}^3$ , respectively), using the multiple regression model, can not be predicted by the variables of porosity level (P, %), surface roughness (R<sub>a</sub>, μm), crystallinity (DOC, %) and residual stress (σ, MPa), because their units are different and, therefore, the regression coefficients cannot be compared. Therefore, the normalized values of the variables were used. The results of multiple regressions of  $C_{\text{Ca}}^1$  and  $C_{\text{Ca}}^3$  with respect to the normalized variables are as follows:

$$C_{\text{Ca}}^1 = 3.20 - 0.20[\text{DOC}]^* + 0.32[R_a]^* + 0.27[P]^* + 0.32[\sigma]^* \quad (3)$$

$$C_{\text{Ca}}^3 = 4.06 - 0.31[\text{DOC}]^* + 0.14[R_a]^* + 0.10[P]^* + 0.01[\sigma]^* \quad (4)$$

The regression coefficients of equations 3 and 4 reveal that the calcium concentration after 1 or 3 days incubation increases with increasing residual stress, porosity level and surface roughness, and decreasing the crystallinity of the HA coatings. The coefficients of equations 3 and 4 indicate that the solubility of HA coatings after 1 and 3 days immersion in SBF solution is controlled by the coating characteristics in order residual stress ≥ roughness > porosity > crystallinity and crystallinity > roughness > porosity > residual stress, respectively. The comparison of each variable coefficient for 1 day immersion with its value for 3 days indicates that the

residual stress significantly influenced the dissolution behavior at early times of immersion. It is noted that the residual stress affects the equilibrium thermodynamics of HA, and can alter the equilibrium concentrations of supernatant ionic species in solution. It is believed that the tensile stresses in HA coatings enhance dissolution [8]. The constant terms in equations 1 and 2 can be considered as the calcium concentrations released from an amorphous, dense coating with a zero stress, and a smooth surface.

The results indicate that the coatings with a higher residual stress would be expected to release excessive levels of calcium ions at initial stages of immersion in SBF solution. Therefore, the tensile residual stress in the HA coatings can significantly influence the rate of dissolution at initial stages of contact with body fluid, which may lead to adverse effects on living bone cells. Furthermore, the tensile stress is reported to promote multiple cracking of the coatings [8]. These facts indicate that it would be desirable for both promoting a rapid integration and long-term stability to produce coatings with a low tensile residual stress, or under zero stress conditions.

## I. CONCLUSION

The plasma sprayed HA coatings with different crystallinities, residual stresses, porosity levels and surface roughness values were produced using various process parameters, and their calcium dissolution behaviors in SBF were evaluated. The calcium dissolution behaviors of the coatings were determined by a combined effect of the surface roughness, porosity, residual stress and crystallinity. The solubility of coatings was increased with an increase of the porosity, the residual stress and the surface roughness, but decreased with increasing the crystallinity. At initial stages of immersion in SBF solution, the tensile residual stress in the HA coatings results in a significant increase in the rate of dissolution. It is suggested that the plasma sprayed HA coatings with a low tensile residual stress or under zero stress conditions would be desirable for both the early bone apposition and the long-term stability.

## REFERENCES

- [1] L. Sun, C. C. Berndt, K. A. Gross, A. Kucuk, "Materials fundamental and clinical performance of plasma-sprayed hydroxyapatite coatings", *J Biomed Mater Res*; vol. 58, pp. 570–592, 2001.
- [2] K. A. Gross, W. Walsh, E. Swarts, "Analysis of retrieved hydroxyapatite-coated hip prostheses", *J Thermal Spray Technology*; vol.3, no. 2, pp. 190–199, 2003.
- [3] Y. C. Tsui, C. Doyle, T. W. Clyne, "Plasma sprayed hydroxyapatite coatings on titanium substrates Part 1: Mechanical properties and residual stress levels", *Biomaterials*; vol. 9, pp. 2015–2029, 1998.
- [4] O. Grafmann, R. B. Heimann, "Compositional and microstructural changes of engineered plasma-sprayed hydroxyapatite coatings on Ti6Al4V substrates during incubation in protein-free simulated body fluid", *J Biomed Mater Res*; vol. 53, pp. 685–693, 2000.
- [5] L. Chou, B. Marek, W. R. Wagner, "Effects of hydroxyapatite coating crystallinity on biosolubility, cell attachment efficiency and proliferation in vitro", *Biomaterials*; vol. 19, pp. 977–985, 1999.
- [6] L. Sun, C. C. Berndt, K. A. Khor, H. N. Cheang, K. A. Gross, "Surface characteristics and dissolution behavior of plasma-sprayed hydroxyapatite coating", *J Biomed Mater Res*, vol. 62, pp. 228–236, 2002.
- [7] J. Weng, L. Quing, J. G. C. Wolke, X. Zhang, K. de Groot, "Formation and characteristics of the apatite layer on plasma-sprayed hydroxyapatite coatings in simulated body fluid", *Biomaterials*; vol.18, pp.1027–1035, 1997.
- [8] V. Sergio, O. Sbaizer, D. R. Clarke, "Mechanical and chemical consequences of the residual stresses in plasma-sprayed hydroxyapatite coatings", *Biomaterials*, vol.18, pp. 477–482, 1997.
- [9] Y. C. Yang, E. Chang, "Influence of residual stress on bonding strength and fracture of plasma-sprayed hydroxyapatite coatings on Ti-6Al-4V substrate" *Biomaterials*; vol. 22, pp. 1827–1836, 2001.
- [10] C. E. Mancini, C. C. Berndt, L. Sun, A. Kucuk, "Porosity determinations in thermally sprayed hydroxyapatite coatings" *J Mat Sci*, vol.36, pp. 3891–3896, 2001.
- [11] D. B. Marshall, B. R. Lawn "Indentation technique for measuring stresses in tempered glass surfaces", *J Am Ceram Soc*, vol.; 60, pp. 86–87, 1977.
- [12] A. G. Evans, E. A. Charles, "Fracture toughness determination by indentation", *J Am Ceram Soc*, vol.; 59, pp. 371–372, 1976.
- [13] L. Sun, C. C. Berndt, C. P. Grey, "Phase, structural and microstructural investigations of plasma sprayed hydroxyapatite coatings", *Materials Science and Engineering A*, vol. 360, pp.70–84, 2003.
- [14] S. Guessasma, G. Montavon, C. Coddet, "Modeling of the APS plasma spray process using artificial neural networks: basis, requirements and an example" *Computational Materials Science*, vol. 29, pp. 315–333, 2004.
- [15] T. Valente, C. Bartuli, M. Sebastiani, F. Casadei, "Finite element analysis of residual stress in plasma-sprayed ceramic coatings", *Proc Instn Mech Engrs Part L: J Materials: Design and Applications*, vol. 218, pp. 321–330, 2004.